

The Selection of Optimum Conditions in HPLC

I. The Determination of External Band Spreading in LC Instruments*

H. H. Lauer**/G. P. Rozing

Hewlett-Packard GmbH, Hewlett-Packard-Straße, D-7517 Waldbronn-2, FRG

Key Words

External band broadening
Calculation methods
Small-bore columns
High-performance liquid chromatography

Summary

A new equation which describes the interdependence of instrument band spreading, injection volume and input profile is proposed and experimentally verified in two modes: 1. without a column; 2. with a column.

It is shown that under equivalent conditions both modes are in excellent agreement. The method of calculation of the variance of a response function appeared to be of utmost importance in correctly interpreting the experimentally observed interdependence of instrumental band spreading and injection characteristics.

Introduction

The use of small volume, high efficiency columns puts heavy demands on instrument design and its constituent parts such as sampling system, detector, connecting tubing, fittings, amplifier time constants and data acquisition devices.

Hydrodynamically, external band spreading is mainly caused in flow-through sub-systems of a chromatographic instrument whereas improper handling of analogue data or insufficient analogue-to-digital sampling rates cause temporarily incorrect representation of the responding signals. The former will seriously affect separation performance and detection limits which can be achieved by very efficient, small volume columns. Its relative and absolute magnitude are therefore of utmost importance to instrument design and have been the subject of investigation in a large number of papers [1–12].

The theoretical basis stems from the paper on the mathematical treatment of the response of independent sub-systems to different input functions by Sternberg [1]. Al-

though the above mentioned investigations provided the chromatographer with sufficient insight into the phenomenon and causes of external band spreading they obscured an unambiguous and rigid description of the latter for two reasons:

- by assuming that the chromatographic sub-systems are mutually independent;
- by using methods to calculate variances of response functions which are not accurate and therefore violate the assumptions in the mathematical model as treated by Sternberg [1].

In this paper the additivity of variances of response functions generated in chromatographic sub-systems is re-investigated together with the influence of the applied calculation method on the output functions obtained.

Theoretical

The determination of external band spreading in a chromatographic system can be performed in two ways:

- without a column in the system. We call this *the short circuited mode*;
- with a column in the system. We call this *the normal mode*.

The short circuited mode

Basically the shape of the response function to an excitation of the chromatographic system (concentration signal) is determined by the shape of the input function and the shape of the pulse response of the system [1, 13].

In mathematical terms, the variance of the output function is the sum of the variances of the input signal, $\sigma_{V(inj)}^2$, and the pulse response of the system $\sigma_{V(0)}^2$ (Fig. 1)

$$\sigma_{V(ext)}^2 = \sigma_{V(inj)}^2 + \sigma_{V(0)}^2 \quad (1)$$

For a well defined injection volume, V_{inj} , the variance can be calculated as the second normalized central moment M_2 . For example, the volume variance of a rectangular input function is given by $V_{inj}^2/12$ whereas for a Gaussian input function the variance is given by $V_{inj}^2/2\pi$. In this case the volume standard deviation is $V_{inj}/\sqrt{2\pi}$ and can be calculated from the half width at 0.607 of the peak height of the Gaussian input function.

Calculating the volume standard deviation of a rectangular function in this way, which we will call the 'hand' method,

* Presented as part of a poster at the Vth International Symposium on Column Liquid Chromatography, Avignon (France), 11–15 May 1981.

** Author to whom correspondence should be sent.

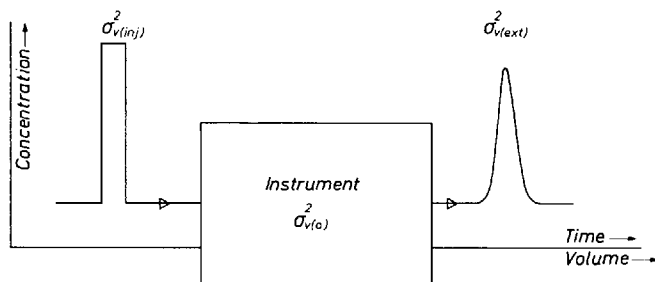


Fig. 1 Model representation of bandbroadening in short circuited mode.

necessarily leads to inaccurate values of the variance. Moreover it will be clear that the 'hand' method provides values of the variance which are strongly dependent on the peak shape, whereas the second normalized central moment always represents the variance of a signal correctly.

Taking the shape of the input signal into account we can rewrite (1) as

$$\sigma_{v(\text{ext})}^2 = \frac{V_{\text{inj}}^2}{D^2} + \sigma_{v(0)}^2 \quad (2)$$

in which D^2 is the normalization factor depending on the peak shape of the input signal and the calculation method. Table I summarizes the values of D^2 for the above mentioned peak shapes.

Table I. Values of D^2 for different calculation methods on input functions with different shapes

Input function Calc. method	Rectangular	Gaussian
	Moments	12
'hand'	4	2π

From eq. (2) it is expected that if the basic hypothesis is correct a plot of $\sigma_{v(\text{ext})}^2$ versus V_{inj}^2 would provide a linear function with slope $1/D^2$ and the variance of the impulse response of the instrument, $\sigma_{v(0)}^2$, as the axis intercept.

Normal mode

In this case (Fig. 2) the variance of the output function, $\sigma_{v(\text{tot})}^2$, can be written as

$$\sigma_{v(\text{tot})}^2 = \sigma_{v(\text{ext})}^2 + \sigma_{v(\text{col})}^2 \quad (3)$$

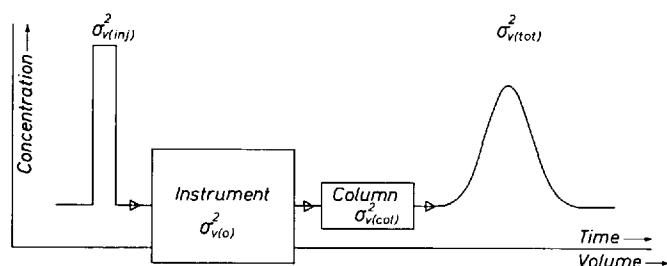


Fig. 2 Model representation of bandbroadening in chromatographic system.

With (2), (3) is transformed in

$$\sigma_{v(\text{tot})}^2 = \frac{V_{\text{inj}}^2}{D^2} + \sigma_{v(0)}^2 + \sigma_{v(\text{col})}^2 \quad (4)$$

in which $\sigma_{v(\text{col})}^2$ is the volume variance of the impulse response of the column. In order to evaluate $\sigma_{v(\text{ext})}^2$ from (3) $\sigma_{v(\text{col})}^2$ has to be known. This volume variance can be calculated from (5)

$$\sigma_{v(\text{col})}^2 = \frac{\epsilon_t V_{\text{col}} (1 + k')}{N_{\text{col}}^{1/2}} \quad (5)$$

where ϵ_t , V_{col} , k' and N_{col} are the total porosity of the column bed, the column volume, the capacity factor and the number of theoretical plates generated by the column respectively. The values of ϵ_t , V_{col} and k' can be obtained with fair accuracy for any column.

However, the determination of N_{col} is more painstaking because only $\sigma_{v(\text{tot})}^2$ is observed from which only N_{obs} can be evaluated which is necessarily made up by $\sigma_{v(\text{col})}^2$ and $\sigma_{v(\text{ext})}^2$ (eq. (3)). To solve this problem two approaches can be applied:

1. if $\sigma_{v(\text{ext})}^2 \ll \sigma_{v(\text{col})}^2$ which is achieved when $V_{\text{inj}} \rightarrow 0$ and/or with large values of k' or V_{col} then $N_{\text{obs}} = N_{\text{col}}$;
2. by plotting the observed variance, $\sigma_{t(\text{tot})}^2$, of the obtained response functions versus the retention times squared, t_{R}^2 , for a certain number (n) of eluted compounds [14].

This approach is elucidated by rewriting eq. (3) in time units

$$\sigma_{t(\text{tot})}^2 = \sigma_{t(\text{ext})}^2 + \sigma_{t(\text{col})}^2 \quad (6)$$

With

$$\sigma_{t(\text{col})}^2 = \frac{t_{\text{R}}^2}{N_{\text{col}}} \quad (7)$$

t_{R} being the retention time of an eluted component, eq. (6) is transformed into

$$\sigma_{t(\text{tot})}^2 = \sigma_{t(\text{ext})}^2 + \frac{t_{\text{R}}^2}{N_{\text{col}}} \quad (8)$$

A plot of $\sigma_{t(\text{tot})}^2$ versus t_{R}^2 , according to eq. (8), should be a linear function with axis intercept $\sigma_{t(\text{ext})}^2$ and slope $1/N_{\text{col}}$. By varying V_{inj} , its influence on $\sigma_{v(\text{ext})}^2$ can be investigated with eq. (4) and compared with the results from the short circuited mode by using the same two calculation methods. The underlying assumptions for the above mentioned second approach will be discussed later.

Experimental

Apparatus, Chemicals and Materials

A Hewlett-Packard 1084 B Analytical High-Pressure Liquid Chromatograph was modified to reduce the external dead volume (which included injection system, tubing, fittings and detector cell) to less than 15 mm^3 by using stainless steel (316) tubing with 0.15 and 0.10 mm i.d. and $\frac{1}{16}$ " o.d., zero dead volume fittings (Swagelok $\frac{1}{16}$ ") and a detector cell of 4.0 mm^3 .

The time constant (time required to rise from 10–90%) of the detector signal board was changed from 200ms to 10ms. The analogue signals produced by the variable wavelength detector of the instrument were digitized by a HP 18652A A/D converter and transferred to a HP 3356A datasystem which operated at a sampling rate of 8 Hz. The moments, retention times and half-widths at 0.607.x height were calculated by a series of programs, written in Lab Basic.

Acetonitrile (p.A. grade; E. Merck, FRG) and water (distilled and deionized) were premixed in the eluent bottle. ODS Hypersil® (5 µm) was used as the stationary phase in a stainless steel (316) column of 100 x 2.0mm equipped with low dead volume (< 1.5mm³) fittings containing porous stainless steel (316) frits with an average pore diameter of 2µm (Mott Metallurgical Corp., USA). In the short circuited mode the sample consisted of 0.1% (w/v) diethylphthalate (GC-grade; E. Merck) dissolved in the mobile phase. In the normal mode a 5 components sample (phenol, benzonitrile, nitrobenzene, 2-chloronitrobenzene and toluene all GC-grade, Chem. Service, PA, USA, and approximately 0.1% w/v per component, except toluene which was 1% w/v) dissolved in the mobile phase was used. Curve fitting of a second order equation was performed with a HP-85 programmable desk top calculator.

Results and Discussion

Short Circuited Mode; Application of the Moment Method

In these experiments the column was removed from the chromatographic system and replaced by a normal zero dead volume fitting ($\frac{1}{16}$ " Swagelok). The mobile phase, water/acetonitrile (60/40% v/v) was run at calibrated flows of 0.13, 0.53, 1.22 and 2.57 cm³/min respectively. At each flow the injection volume was varied from 2 to 4, 8, 16, 25, 40, 60 and 90 mm³.

From the signal obtained the moments were calculated by the Lab Data System in time units. The volume variances were calculated by multiplication of the second normalized central moment, M_2 , with the square of the flow rate. Table II summarizes the experimental data points.

Table II. Experimental data points (statistical moments; short circuited mode)

Flow	0.13 $\frac{\text{cm}^3}{\text{min}}$		0.53 $\frac{\text{cm}^3}{\text{min}}$		1.22 $\frac{\text{cm}^3}{\text{min}}$		2.57 $\frac{\text{cm}^3}{\text{min}}$	
V_{inj}^2 (mm ⁶)	$\sigma_{v(EXT)}^2$ (mm ⁶)	D^2	$\sigma_{v(EXT)}^2$ (mm ⁶)	D^2	$\sigma_{v(EXT)}^2$ (mm ⁶)	D^2	$\sigma_{v(EXT)}^2$ (mm ⁶)	D^2
4	15.69	1.01	49.86	2.24	—	—	—	—
16	27.56	1.01	55.22	2.24	94.5	1.10	176.3	0.98
64	45.33	1.91	72.07	2.67	103.2	2.76	215.1	1.16
256	82.6	3.61	129.9	3.13	192.1	2.28	336.4	1.45
625	134.9	5.07	172.2	5.04	232.5	4.10	409.5	2.51
1600	245.1	6.86	295.6	6.46	356.8	5.78	586.8	3.75
3600	466.3	7.92	513.2	7.74	560.9	7.49	840.1	5.29
8100	906.1	9.06	998.0	8.53	1029.4	8.53	1400.6	6.53

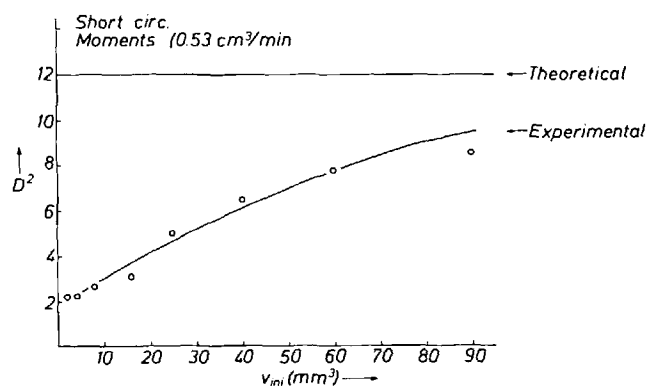


Fig. 3
Dependence of D^2 -factor on injection volume.

If the basic hypothesis (eqs.(1) and (2)) is correct, that is, the variance of the output function is the sum of the variances of the input signal, V_{inj}^2/D^2 , and the impulse response of the system, $\sigma_{v(0)}^2$, and we assume that we can estimate $\sigma_{v(0)}^2$ by graphical extrapolation of $\sigma_{v(EXT)}^2$ to $V_{inj}^2 = 0$ the calculated value of D^2 from eq. (2) should be a constant for all injected sample volumes and should have the theoretical value of 12. Table II and Fig. 3 clearly show that this is not the case but on the contrary reveal that D^2 or D is a function of V_{inj}^2 resp. V_{inj} . Although this result also was obtained by previous workers [15–21] and calls for evaluation of the dependence of D^2 and/or $\sigma_{v(EXT)}^2$ on V_{inj} so far this has not been described.

As in all cases the calculated D^2 -factor is smaller than the theoretical value and appears in the denominator of the first term in eq.(2), it can be argued that if we stick to the original hypothesis the measured $\sigma_{v(EXT)}^2$ is larger than is expected by relation (2). So one has to account for an additional broadening in the basic eq. (2). Therefore other possible correlations between the experimental data were considered.

Two converging regressions of the data in Table II were obtained. Second order non-linear regression of the type $y = a_0 + a_1 x + a_2 x^2$ in which $y = \sigma_{v(EXT)}^2$ and $x = V_{inj}$ and linear regression of the type $y = b_0 + b_1 x$ in which $y = \sigma_{v(EXT)}$ and $x = V_{inj}$. The results are summarized in Tables III and IV and Figs. 4 and 5. In particular the second order regression (Table III) shows a very high non-linear correlation

Table III. Values resulting from second order regression of $\sigma_{v(EXT)}^2, V_{inj}$ on entire set of data pairs as in Table II

Flow ($\frac{\text{cm}^3}{\text{min}}$)	a_0 (= $\sigma_{v(0)}^2$) (mm ⁶)	a_1 (mm ⁶)	a_2 (= $\frac{1}{D^2}$)	r	S_{yx}^{n-2} (mm ⁶)	$\frac{S_{yx}^{n-2}}{y_{obs}}$ (%)	n
0.13	15.27	2.69	0.0800	0.99993	4.0	1.7	8
0.53	47.87	2.73	0.0865	0.99972	8.4	3.0	8
1.22	84.66	3.84	0.0732	0.99891	17.1	4.7	8
2.57	163.64	7.86	0.0643	0.99899	22.1	3.9	8

n: number of data pairs

coefficient and a low relative scatter of the experimental datapoints. It is easily calculated that $\sqrt{a_0} \approx b_0$ and that $\sqrt{a_2} \approx b_1 \approx 1/D$.

This leads to the following, experimentally based, equations

$$\sigma_{v(\text{ext})} = \sigma_{v(0)} + \frac{V_{\text{inj}}}{D} \quad (9a)$$

and

$$\sigma_{v(\text{ext})}^2 = \left(\sigma_{v(0)} + \frac{V_{\text{inj}}}{D} \right)^2 = \sigma_{v(0)}^2 + \frac{2\sigma_{v(0)}V_{\text{inj}}}{D} + \frac{V_{\text{inj}}^2}{D^2} \quad (9b)$$

in which $\sigma_{v(0)}^2$ represents the variance of the impulse response of the system which, by definition, equals $\sigma_{v(\text{ext})}^2$ for zero injection volume, V_{inj}^2/D^2 represents the variance of the input signal and the cross term $2\sigma_{v(0)}V_{\text{inj}}/D$ represents

Table IV. Values resulting from linear regression of $\sigma_{v(\text{ext})}$, V_{inj} (statistical moments; short circuited mode)

Flow ($\frac{\text{cm}^3}{\text{min}}$)	b_0 ($=\sigma_{v(0)}$) (mm^3)	b_1 ($=\frac{1}{D}$)	D	r	\hat{S}_{yx}^{n-2} (mm^3)	$\frac{\hat{S}_{yx}^{n-2}}{\bar{y}^{\text{obs}}}$ (%)	n
0.13	4.05	0.2915	3.43	0.99925	0.38	2.9	8
0.53	6.39	0.2770	3.61	0.99935	0.33	2.3	8
1.22	8.73	0.2571	3.89	0.99768	0.60	3.4	8
2.57	13.00	0.2725	3.67	0.99677	0.62	2.9	8

Table V. $\sigma_{v(0)}$ and D-values calculated from coefficients a_0 and a_2 as summarized in Table III

Flow (cm^3/min)	$\sigma_{v(0)}$ (mm^3)	D
0.31	3.91	3.54
0.53	6.92	3.40
1.22	9.20	3.70
2.57	12.79	3.94

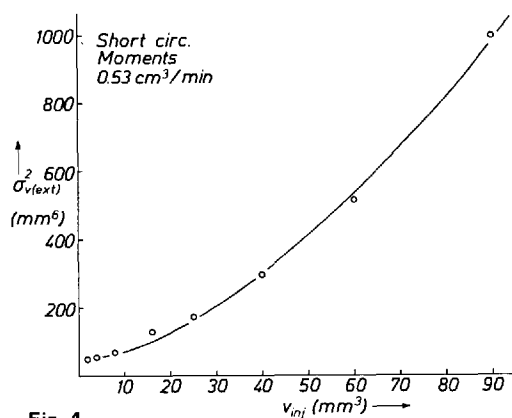


Fig. 4

Dependence of volume variance of response function on injection volume in short circuited mode by applying statistical moments.

the additional broadening caused by the interdependence of instrumental broadening and the width of the input function. In qualitative terms, it can be interpreted that the effect of instrumental broadening is more severe for small than for large injection volumes.

Moreover the high convergence of these regressions is also reflected in the close agreement of the calculated D- and $\sigma_{v(0)}$ -values as shown in Tables IV and V. The appearance of eq. (9) is as well supported by the experiments of Kirkland et al. [10].

Application of the 'Hand' Method

The experimental volume variances of the response functions are now calculated from the width at 0.607 of the peak height. The data are summarized in Table VI. Proceeding as before, that is, to estimate $\sigma_{v(0)}^2$ from graphical extrapolation of $\sigma_{v(\text{ext})}^2$ to $V_{\text{inj}}^2 = 0$, the calculated value of D^2 appears more or less constant and approaches the value of 4 which was predicted in Table I. Therefore it seems as if the theoretical relation (2) indeed is experimentally confirmed.

Table VI. Experimental data points ('hand' method; short circuited mode)

Flow	0.13 $\frac{\text{cm}^3}{\text{min}}$		0.53 $\frac{\text{cm}^3}{\text{min}}$		1.22 $\frac{\text{cm}^3}{\text{min}}$		2.57 $\frac{\text{cm}^3}{\text{min}}$	
	V_{inj}^2 (mm^6)	$\sigma_{v(\text{ext})}^2$ (mm^6)	$\sigma_{v(\text{ext})}^2$ (mm^6)	D^2	$\sigma_{v(\text{ext})}^2$ (mm^6)	D^2	$\sigma_{v(\text{ext})}^2$ (mm^6)	D^2
4	10.94	—	25.00	—	22.28	—	—	—
16	14.45	3.84	27.67	5.53	24.78	5.08	61.70	—
64	25.39	4.24	34.34	6.69	33.68	5.31	81.70	2.40
256	62.26	4.93	70.22	5.63	66.95	5.65	122.70	3.78
625	148.7	4.51	140.9	5.38	137.2	5.41	193.0	4.53
1600	370.5	4.44	347.1	4.96	334.9	5.11	406.1	4.56
3600	832.3	4.38	780.1	4.77	772.6	4.79	885.6	4.33
8100	1873.7	4.35	1788.4	4.59	1761.8	4.65	1936.0	4.31

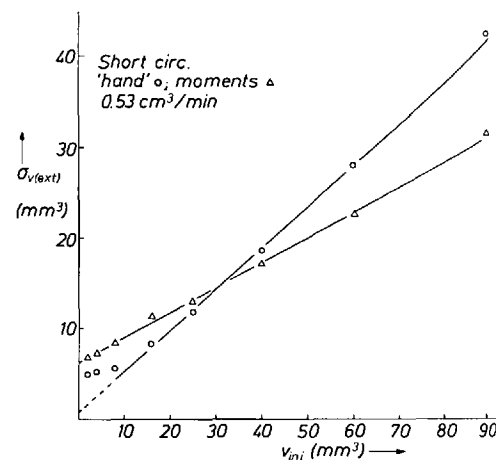


Fig. 5

Dependence of volume standard deviation of response function on injection volume in short circuited mode by applying 'hand' method and statistical moments.

Fitting a least square parabola of the previous type to these data resulted in Table VII in which the values for $\sigma_{v(0)}$ and D , calculated from a_0 and a_2 , are also shown.

The overall relative scattering of the data is very small and a perfect non-linear correlation is exhibited in this table. The calculated D -values are remarkably close to the theoretical value.

Again a possible linear relationship between $\sigma_{v(ext)}$ and V_{inj} was investigated and shown in Fig. 5 for a flow of 0.53 cm^3/min . From this figure it is clear that the assumed relationship starts at an injection volume of approximately 8 mm^3 . All other flows show the same trend. Fitting a least square line to the obtained data (omitting those at 2 and 4 mm^3) resulted in the characteristic values shown in Table VIII. The overall relative scattering of the data is small and the linear correlation extremely high. In this case the calculated D -values show the largest average deviation from the theoretical value.

In contradiction to the regression results obtained from statistical moments (Tables III and IV) here the regression-coefficients show an inconsistent picture and moreover a negative coefficient a_1 is obtained.

Normal Mode

In this experiment the tubings from injection system and detector were connected to a 100 x 2.0mm column packed with ODS Hypersil® (5 μm) (Fig. 2). A mobile phase of water/acetonitrile (60/40% v/v) was run at 0.54 cm^3/min through the instrument and the mixture of 5 components was injected with varying volumes.

Table VII. Values resulting from second order regression on data pairs calculated by 'hand' method (short circuited mode)

Flow ($\frac{\text{cm}^3}{\text{min}}$)	$\sigma_{v(0)}$ (= $\sqrt{a_0}$) (mm^3)	D (= $\sqrt{1/a_2}$)	a_1	r	\hat{S}_{yx}^{n-2} (mm^6)	$\frac{\hat{S}_{yx}^{n-2}}{\bar{y}^{obs}}$ (%)	n
0.13	3.39	2.07	-0.39	1.00000	1.6	0.4	8
0.53	5.44	2.08	-1.37	0.99999	2.2	0.6	8
1.22	5.21	2.09	-1.37	0.99999	2.9	0.7	8
2.57	8.32	2.03	-1.02	0.99995	7.4	1.4	8

Table VIII. Values resulting from linear regression of $\sigma_{v(ext)}$, V_{inj} . Data pairs for $V_{inj} = 2$ and 4 mm^3 omitted ('hand' method; short circuited mode)

Flow (cm^3/min)	$\sigma_{v(0)}$ (= b_0) (mm^3)	D (= $1/b_1$)	r	\hat{S}_{yx}^{n-2} (mm^3)	$\frac{\hat{S}_{yx}^{n-2}}{\bar{y}^{obs}}$ (%)	n
0.13	0.64	2.12	0.99969	0.40	2.1	6
0.53	1.24	2.22	0.99885	0.74	3.9	6
1.22	1.12	2.23	0.99871	0.78	4.1	6
2.57	4.01	2.39	0.99676	1.21	5.7	6

Determination of the theoretical plate number (N_{col})

At constant linear velocity (u_0), particle size (d_p), mobile phase composition, temperature and column bed geometry, the theoretical plate number (N_{col}) is still a function of the capacity factor (k') and the diffusion coefficients of a certain solute in the mobile (D_m) and stationary phase (D_p) [22-25].

Neglecting the k' dependence [26-28] and selecting a number of components which, under the constant conditions mentioned before, are completely separated on the column and have virtually equal diffusion coefficients in the mobile phase, eq. (8) will be sufficiently accurate to determine N_{col} if it is further assumed that D_m equals D_p . According to eq. (8) a value for the external bandspreading, $\sigma_{v(ext)}$, can be obtained for every injection volume by applying the suggested linear regression.

For both calculation methods the results are summarized in Table IX. As at an injection volume of 90 mm^3 a complete separation of all components was no longer observed, the corresponding values are omitted from this table. At each injection volume the regression of $\sigma_{t(tot)}^2$, t_R^2 shows for both calculation methods a good linear correlation together with a fairly constant value of the regression coefficient b_1 ($= 1/N_{col}$).

However, in using statistical moments a larger relative scattering, $\hat{S}_{yx}^{n-2}/\bar{y}^{obs}$, is observed. The values of $\sigma_{v(ext)}$ obtained are also in fair agreement with the values obtained in the short circuit mode (Tables II and VI).

Again, first the validity of eq. (2) was checked as described before and the same results were obtained. In using statistical moments the calculated D values are not constant but a

Table IX. Values resulting from least square fit according to eq. (8) for various injection volumes

Calc. method	V_{inj} (mm^3)	$\sigma_{v(ext)}$ (mm^3)	D^2	N_{col}	r	\hat{S}_{yx}^{n-2} (s^2)	$\frac{\hat{S}_{yx}^{n-2}}{\bar{y}^{obs}}$ (%)
m	2	6.91	-	5859	0.99250	0.36	11.7
m	4	7.60	1.20	5287	0.99435	0.34	9.9
m	8	9.02	1.73	4862	0.99335	0.41	10.2
m	16	11.97	2.59	4716	0.99059	0.50	10.3
m	25	15.06	3.44	4553	0.98472	0.66	11.0
m	40	19.70	4.66	4274	0.97949	0.69	8.4
m	60	25.88	5.76	3928	0.96362	1.21	10.0
				$\bar{N} = 4783$			
				$S_N/\bar{N} = 13.4\%$			
h	2	4.95	-	5423	0.99889	0.15	5.0
h	4	5.47	2.21	5237	0.99928	0.12	3.9
h	8	6.83	2.67	5136	0.99927	0.13	3.7
h	16	9.80	3.49	4974	0.99879	0.17	4.1
h	25	13.92	3.65	4906	0.99863	0.18	3.4
h	40	21.52	3.63	5147	0.99725	0.25	2.9
h	60	33.28	3.32	6371	0.98168	0.53	3.3
h = 'hand' method				$\bar{N} = 5313$			
m = moments				$S_N/\bar{N} = 9.3\%$			

* Calculated from $[\sigma_{t(ext)}]_{t_R=0}$ and multiplying with F (volume flow rate)

function of $V_{inj}(V_{inj}^2)$, whereas using 'hand' calculation a fairly constant value of the D^2 -factor close to its theoretical value, 4, is observed (Table IX).

The second order regression of $\sigma_{v(ext)}$, V_{inj} and the linear regression of $\sigma_{v(0)}$, V_{inj} , using the experimental data points obtained by calculating statistical moments, both again show a converging picture (Table X). The regression constants $\sigma_{v(0)}$ and D obtained by the individual regressions are virtually identical.

Using experimental data points obtained by 'hand' calculation, diverging results are obtained after regression (disagreement between $\sigma_{v(0)}$ -values and negative coefficient a_1), showing again the inadequacy of this method to properly describe variances of transient skewing signals (Table X).

The results obtained from the short circuited and normal mode are compared in Table XI.

The agreement between both modes at the investigated flow-rate is very striking. A general application of determining external bandspreading in the normal mode as suggested by the plotting procedure of eq. (8) still needs more experimental evidence under different conditions.

Table X. Values resulting from different types of regression analysis on data pairs from Table IX calculated by different methods. Normal mode; flow 0.54 cm³/min

Calc. method	Regr. type	$\sigma_{v(0)}$ (mm ³)	D	a_1	r	$\frac{S_{yx}^{n-2}}{mm^3 (mm^6)}$	$\frac{S_{yx}^{n-2}}{\bar{y}^{obs}}$ (%)	n
m	linear	6.47	3.05	—	0.99935	0.28	2.0	7
m	sec. order	5.91	3.41	5.43	0.99997	(1.80)	0.8	7
h	linear	1.80	1.95	—	0.99718	0.92	5.4	5*
h	sec. order	6.05	1.73	-2.28	0.99969	(10.8)	3.8	7

* data pairs for $V_{inj} = 2$ and 4 mm^3 omitted.

Table XI. Comparison of results obtained from short circuited and normal modes

Mode	Calc. method	Flow ($\frac{cm^3}{min}$)	Regr. type	$\sigma_{v(0)}$ (mm ³)	D	r	$\frac{S_{yx}^{n-2}}{\bar{y}^{obs}}$ (%)	n
s	m	0.53	linear	6.39	3.61	0.99935	2.3	8
n	m	0.54	linear	6.47	3.05	0.99935	2.0	7
s	m	0.53	sec. order	6.92	3.40	0.99972	3.0	8
n	m	0.54	sec. order	5.91	3.41	0.99995	0.8	7
s	h	0.53	linear	1.24	2.22	0.99885	3.9	6
n	h	0.54	linear	1.80	1.95	0.99718	5.4	5
s	h	0.53	sec. order	5.44	2.08	0.99999	0.6	8
n	h	0.54	sec. order	6.05	1.73	0.99939	3.8	7

s: short circuited mode, n: normal mode.

Comparison of both calculation methods

In using true variances of response functions, calculated by means of the second moment (M_2), it is obvious that eq. (2) is not sufficiently accurate to describe external bandspreading. If inaccurate variances calculated by the 'hand' method are applied, however, eq. (2) appears to be fairly accurate which in itself is very remarkable and probably accounts for its prolonged use by chromatographers.

Both calculation methods provide data which are very accurately described by eq. (9a) although those obtained by the 'hand' method show some significant deviations in their best fit:

1. the constants $a_1 = 2\sigma_{v(0)}/D$ have negative absolute values for all investigated flows and therefore are probably physically meaningless;
2. a non-linear relationship between $\sigma_{v(0)}$ and V_{inj} for injection volumes smaller than 8 mm^3 leading to a disagreement between the $\sigma_{v(0)}$ -values obtained from linear and second order regression.

This clearly shows that values for external bandspreading obtained from handling of data calculated by the 'hand' method are very suspect. D-values obtained from 'hand' method data are hardly dependent on the investigated equations whereas those from second moment data are. Their respective magnitudes are in accordance with the predicted theoretical figures and indicate that in the short circuited mode the injection profile virtually approaches a slug. If the latter, however, is neither a slug nor Gaussian significant information on its shape can only be obtained by using statistical moments.

Conclusions

A new eq. (9) which accounts for the mutual dependence of instrument bandspreading, injection volume and input profile is proposed.

The absolute value of the instrument bandspreading for $V_{inj} \rightarrow 0$, largely depends on the calculation method applied and can be evaluated both in a short circuited and normal mode. The former mode clearly showed a flow dependence of the investigated parameter which should therefore also be examined in the normal mode together with changes in external volume (such as lengths and inside diameter of tubing and detector cell volumes).

Response functions are completely described by their statistical moments which therefore should always be applied if transport phenomena are investigated.

The experimentally obtained injection profile value, D , shows that for different flow rates and injection volumes the applied sampling system virtually produces a slug.

The column evaluation method, as suggested in this paper, needs more experimental evidence and should be investigated under totally different conditions.

Acknowledgement

The assistance of Wolfgang Kretz (injection hardware), Hans Georg Haertl (column hardware and program software), Gerard Plé (electronical hardware) and Peter Pion (column packing and evaluation) is highly appreciated. The authors thank Mrs. Johanna Lauer for typing the manuscript and the managing director of Hewlett-Packard Waldbronn for permission to publish this paper.

List of Symbols

a_0, a_1, a_2	Coefficients of the parabolic equation applied in the curve fitting of the data pairs
b_0, b_1	Coefficients of the linear equation applied in the curve fitting of the data pairs
D	Factor depending on input profile and calculation method
D_m	Diffusion coefficient of a solute in the mobile phase
D_p	Average diffusion coefficient of a solute in a particle of the stationary phase
d_p	Average particle diameter of the stationary phase
F	Volume flow rate
k'	Capacity factor
M_0	Zeroth moment
M_1	First normalized moment $\int_0^{\infty} th(t)dt/M_0$
M_2	Second normalized central moment $\int_0^{\infty} (t - M_1)^2 h(t) dt/M_0$
N_{col}	Number of theoretical plates generated by the column
r	Regression coefficient of fitted curves
\hat{s}_{yx}^{n-2}	Modified standard error of estimate for (n-2) degrees of freedom
t_R	Retention time of eluted component
u_0	Linear velocity of an unretained component
V_{col}	Column volume
V_{inj}	Volume of injected sample
\bar{y}^{obs}	Mean value of the dependent variable for different types of regression
$\sigma_{v(ext)}^2$	Volume variance of concentration profile due to injection volume, injection device, tubing and detector (external broadening)

$\sigma_{v(inj)}^2$	Volume variance of concentration profile due to injection volume.
$\sigma_{v(col)}^2$	Volume variance of the impulse response of the column
$\sigma_{v(0)}^2$	Equal to $\sigma_{v(ext)}^2$ for $V_{inj} \rightarrow 0$, impulse response of the instrument
σ_t^2	Time variances of above mentioned concentration profiles
ϵ_t	Total porosity of column bed.

References

- [1] J. C. Sternberg, *Advan. Chromatogr.* **2**, 205 (1966).
- [2] I. Halász, P. Walking, *J. Chromatogr. Sci.* **7**, 129 (1969).
- [3] T. W. Smuts, D. J. Solms, F. A. Van Niekerk, V. Pretorius, *J. Chromatogr. Sci.* **7**, 24 (1969).
- [4] J. J. Kirkland, *J. Chromatogr. Sci.* **7**, 7 (1969).
- [5] J. F. K. Huber, J. A. J. Hulsman, C. A. M. Meyers, *J. Chromatogr.* **62**, 79 (1971).
- [6] J. F. K. Huber, R. van der Linden, E. Ecker, M. Oreans, *J. Chromatogr.* **83**, 267 (1973).
- [7] B. L. Karger, M. Martin, G. Guiochon, *Anal. Chem.* **46**, 1640 (1974).
- [8] M. Martin, C. Eon, G. Guiochon, *J. Chromatogr.* **108**, 229 (1975).
- [9] A. Wehrli, K. Hermann, J. F. K. Huber, *J. Chromatogr.* **125**, 59 (1976).
- [10] J. J. Kirkland, W. W. Yau, H. J. Stoklosa, C. H. Dilks, Jr., *J. Chromatogr. Sci.* **15**, 303 (1977).
- [11] H. Colin, G. Guiochon, *J. Chromatogr.* **158**, 183 (1978).
- [12] H. Colin, M. Martin, G. Guiochon, *J. Chromatogr.* **185**, 79 (1979).
- [13] J. F. K. Huber, *Instrumentation for HPLC*, J. F. K. Huber, Ed., Elsevier, Amsterdam, 1978, p. 1.
- [14] J. F. K. Huber, personal communication, Institute of Analytical Chemistry, University of Vienna, 1977.
- [15] A. Wehrli, *Z. Anal. Chem.* **277**, 289 (1975).
- [16] B. Coq, G. Cretier, C. Gonnet, J. L. Rocca, *Chromatographia* **11**, 139 (1978).
- [17] B. Coq, G. Cretier, J. L. Rocca, *J. Chromatogr.* **186**, 457 (1979).
- [18] P. Roumeliotis, K. K. Unger, *J. Chromatogr.* **185**, 445 (1979).
- [19] W. Beck, I. Halász, *Z. Anal. Chem.* **291**, 340 (1978).
- [20] R. Endeke, I. Halász, K. Unger, *J. Chromatogr.* **99**, 377 (1974).
- [21] K. P. Hupe, H. H. Lauer, to be published.
- [22] J. F. K. Huber, J. A. R. J. Hulsman, *Anal. Chim. Acta* **38**, 305 (1967).
- [23] J. F. K. Huber, *J. Chromatogr. Sci.* **7**, 85 (1969).
- [24] J. F. K. Huber, *Column Chromatography*, E. Kováts, Ed., *Chimia Supplementum*, Sauerländer, Aarau, 1970, p. 24.
- [25] J. F. K. Huber, *Ber. Bunsenges. Phys. Chem.* **77**, 159 (1973).
- [26] A. B. Littlewood, *Gas Chromatography*, 2nd edn., Academic Press, 1970, p. 214.
- [27] L. R. Snyder, *J. Chromatogr. Sci.* **7**, 352 (1969).
- [28] B. L. Karger, *Modern Practice of Liquid Chromatography*, J. J. Kirkland, Ed., Interscience, New York, 1971, Chapter 1.

Received: July 21, 1981
Accepted: July 29, 1981
D